JOURNAL OF CATALYSIS 91, 25–35 (1985)

Preparation and Properties of Raney Copper Foraminate Catalysts

N. I. ONUOHA, A. D. TOMSETT, M. S. WAINWRIGHT,[1] AND D. J. YOUNG

School of Chemical Engineering and Industrial Chemistry, The University of New South Wales, P.O. Box 1, Kensington, N.S.W. 2033, Australia

Received March 14, 1984; revised August 16, 1984

The factors influencing the rate of extraction and pore development in Raney copper foraminate catalysts have been studied by caustic leaching of particles of a nominally 50 wt% Cu-Al alloy at 313 K. The leaching reaction leads to the selective dissolution of aluminum, and the formation of a porous copper rim around a core of as yet unreacted alloy. The kinetics of the leaching process have been fitted to a shrinking core model which shows that the reaction is initially chemical reaction controlled, but controlled by pore diffusion at longer times. The surface area per unit mass of copper decreases and the mean pore radius increases with extent of extraction, while the pore volume remains essentially constant. This behavior is explained in terms of a mechanism whereby pore spacing is controlled by segregation of copper and aluminium within the alloy at the leach reaction front. This alloy segregation occurs via a mechanism involving boundary diffusion.

INTRODUCTION

Direct hydrolysis of acrylonitrile over copper-based catalysts has largely replaced the homogeneous (sulfuric acid) process for acrylamide synthesis (*1*). Many copper catalysts have been used for this process with Raney copper being predominant. The particle size of the catalyst depends on the contacting method employed, with fine particles being used for batch slurry reactors (*2*) and fluidized beds (*3*). Larger particles are required for fixed bed operation (*4*). In a recent patent (*5*) it has been claimed that partial activation of Raney alloy results in improved catalyst activity for acrylamide synthesis.

The industrial importance of the Raney copper catalyzed hydrolysis of acrylonitrile has led to a number of recent kinetic studies (*6–9*). In these studies Raney copper has been shown to undergo deactivation due to thermal polymerization of acrylamide and to a lesser extent by oxidation of copper by dissolved oxygen (*9*). Deactivation by fouling with polymer has been shown (*9*) to have a marked effect on the pore size distribution and it is thought that pore structure will have a major influence on the performance of Raney copper catalysts in the hydrolysis of acrylonitrile.

Raney catalysts produced by the incomplete extraction of alloy particles have been termed foraminates (*10*). They consist of an extracted rim of active material and a core of unextracted alloy. In a recent study of the preparation of Raney copper–zinc catalysts for methanol synthesis (*11*) it has been shown that incomplete extraction of Cu–Al–Zn alloys with caustic soda solutions can lead to marked changes in surface and pore morphology. In particular, it was shown that the mean pore size increased with increasing extent of extraction.

A related phenomenon has been observed in a companion study on the complete extraction of Cu–Al alloy particles of different sizes (*12*). In that work it was found that the mean pore size increased with particle size. An explanation for this behavior was developed in terms of phase transformation theory. In that description, control of pore spacings, and hence pore sizes, was attributed to solid-state diffusion within the alloy driven by a chemical potential gradient resulting from the leach reac-

[1] To whom correspondence should be addressed.

0021-9517/85 $3.00

tion. The leaching rate slows with time. Larger particles therefore have lower average leaching rates and their larger pores were thereby explained.

It is evident that this description should be applicable also to the formation of foraminate catalysts, where the pore size would be predicted to increase with increasing thickness of active rim. The purpose of this work was to produce Raney copper catalysts with different surface areas and pore sizes by partial extraction, and to verify the applicability of the phase transformation model. The performance of these catalysts in acrylamide synthesis is discussed elsewhere (*13*).

EXPERIMENTAL

Catalyst preparation. An alloy of composition Cu–50.2 wt% Al was prepared by induction melting the required proportions of copper (99.5% pure) and aluminium (99.9% pure), quenching in water and screening to size (*7*). This alloy consists largely of the intermetallic phase $CuAl_2$. The alloy composition used in most experiments was Cu–50.2 wt% Al.

Leaching of 30 g of alloy particles (2.0 to 2.3 mm) in 150 cm^3 of water was conducted in a gas-tight reaction vessel immersed in a thermostatted bath at 313 K. An aqueous solution (40%) of sodium hydroxide was added from a burette at 5 min intervals. Initially 2 cm^3 of caustic solution was added until a cumulative volume of 20 cm^3 was reached. Then 5 cm^3 additions were made until 100 cm^3 had been added and 10 cm^3 additions were made thereafter. This procedure resulted in isothermal (±0.5 K) leaching of the alloy. Caustic additions were terminated at different time periods varying from 40 min to 24 hr (Table 1) in order to produce a range of catalysts with varied depth of caustic attack (aluminium removal). Each catalyst preparation was then washed with water to a pH of 7 and screened under water to remove any fine particles (<2 mm). The extent of extraction was continuously monitored by measuring hydrogen evolution with a wet gas meter.

Catalyst characterisation. Atomic absorption spectroscopic analysis of acid digested samples was used to measure the chemical composition of alloy and catalyst samples.

Total surface areas, pore volumes, and pore diameters were calculated from nitrogen isotherms which were measured at 77.5 K using a Micromeritics 2100 E ORR surface area, pore volume analyser. Samples of Raney copper catalysts were transferred to a glass sample vessel under water and were evacuated at room temperature for 12 hr to remove most of the water. The samples were then evacuated at 423 K for an additional 12 h before measuring the nitro-

TABLE 1

Alloy and Catalyst Compositions for Varying Times of Extraction

Extraction time (min)	Alloy/catalyst composition (wt%)		$\beta = \frac{W_{Al}}{W_{Cu}}$	Mass of Al extracted per g alloy Z	Volume of H_2 evolved (cm^3) at measurement conditions (294 K, 98 kPa)		Extent of Al extraction X_{Al}
	Cu	Al			Stoichiometric	Measured	
0 (alloy)	49.8	50.2	1.01	0	0	0	0
40	55.7	44.3	0.793	0.107	152	155	0.218
70	62.8	37.2	0.593	0.207	291	303	0.418
140	72.8	27.2	0.374	0.316	444	472	0.637
180	79.1	20.9	0.264	0.371	521	529	0.747
1440	98.8	1.2	0.0123	0.496	697	672	1.01

gen adsorption–desorption isotherms. The pore size distributions were determined from the nitrogen desorption isotherms by the procedure of Pierce (*14*) as modified by Dalla Valle (*15*).

INTERPRETATION OF DATA

Foraminates consist of an extracted rim of active metal and a core of unextracted alloy. Although this core is impervious to the reacting species and hence does not provide catalytic activity, it does contribute mass to the catalyst particle. Since it is only the high surface area porous copper in the extracted rim which is active, it is meaningless to express properties on the basis of a unit mass of composite material even though it is on this basis that properties such as surface area and pore volume are measured. Moreover, as will emerge subsequently, the surface properties of the reacted rim vary with the rim thickness itself. It is therefore unhelpful to refer these properties to the original mass of alloy: instead they should be referred to the mass of rim material, thereby reflecting the change in its nature. By using compositional data obtained by chemical analysis of the catalyst and alloy, and a number of assumptions which are defined below, it is possible to convert data obtained on the basis of unit mass of composite material to those applying to the catalytically active rim material.

If we assume that the particles are spherical and that leaching of aluminium occurs quantitatively and progressively then we have a situation as shown in Fig. 1 which represents the classical shrinking core model for particles of constant size. Chemical analysis by atomic absorption spectroscopy of the alloy yields a mass ratio of aluminium to copper which is designated B. The mass ratio of aluminium to copper in the composite material resulting from partial extraction of an alloy sample is designated β.

In this investigation the particles were approximately spherical and were screened to a narrow size range of 2.0 to 2.3 mm diameter. Microscopic examination showed that after extraction the particle size and shape was the same as the original alloy particle. The shell material was strong and remained intact with no fine material being observed in the extracting liquor. Since the particles have approximately spherical geometry and since copper does not dissolve under the extraction conditions, the values of β and B can be used to obtain characteristics of the active porous shell (*13*). These include

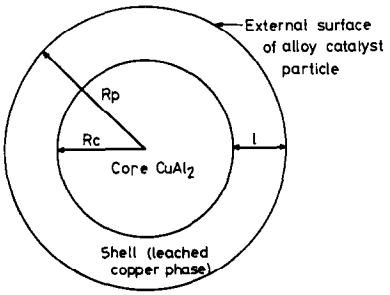

FIG. 1. Idealized shell model of partially leached alloy.

$$\frac{\text{mass of shell}}{\text{mass of composite}} = \frac{M_s}{M_c} = \frac{\left[1 - \frac{\beta}{B}\right]}{[1 + \beta]} \quad (1)$$

and the shell thickness,

$$X = R_p \left[1 - \left(\frac{\beta}{B}\right)^{1/3}\right] \quad (2)$$

where R_p is the particle radius.

Implicit in the development of Eqs. (1) and (2) is the assumption that the aluminium is completely removed from the copper in the shell. However, other studies of completely extracted alloy particles (*16, 17*) show that residual aluminium is present as alumina, leading to values of $\beta \leq 0.02$.

In this work, leaching of the alloy for 24 h at 313 K is expected to lead to complete leaching as confirmed by hydrogen evolution experiments. However, under these conditions a mass ratio of aluminium to copper of 0.0123 was found by chemical analysis. It is assumed that the residual aluminium is evenly distributed throughout the

copper skeleton. Furthermore, it is assumed that the copper shell of the partially leached alloys has the same composition. Applying these assumptions leads to slight modifications to Eqs. (1) and (2) which are then given by:

$$\frac{M_s}{M_c} = \frac{\left[\left(1 - \frac{\beta}{B}\right)\Big/\left(1 - \frac{0.0123}{B}\right)\right]}{[1 + \beta]} \quad (3)$$

and

$$X = R_p\left\{1 - \left[1 - \frac{\left(1 - \frac{\beta}{B}\right)}{1 - \left(\frac{0.0123}{B}\right)}\right]^{1/3}\right\}. \quad (4)$$

The extent of leaching of aluminium for each catalyst was determined from the chemical composition data using the relation

$$Z = \frac{B - \beta}{1 + B} \quad (5)$$

where Z is the mass of aluminium removed per unit mass of starting alloy.

The stoichiometric volumes of hydrogen calculated from Z at the measurement conditions (294 K, 98 kPa) agree closely with the measured hydrogen evolutions (Table 1), indicating that hydrogen evolution takes place quantitatively.

To be able to compare the various properties of the catalysts prepared by varying the duration over which the alloy is leached, it is essential to define a generalized index which unambiguously describes the extent of leaching and which constitutes a basis on which the catalysts could be compared. The leaching process used for catalyst preparation in this work is an example of fluid–particle reactions of the type in which the reacting particle is of unchanging size but of diminishing core. The extent of leaching could therefore be adequately represented by the dimensionless quantity X_{Al}, which is the fractional conversion of the reactant-aluminium in the alloy. At a given instant, X_{Al} is defined by

$$X_{Al} = \frac{\text{mass of Al extracted}}{\text{total mass of Al removable}} = \frac{Z_{(t)}}{Z_{(\text{complete extraction})}} \quad (6)$$

$$= \frac{\text{volume of shell}}{\text{total volume of particle}}. \quad (7)$$

The amount of aluminium leached is related to the volume of hydrogen produced by the stoichiometry of reaction

$$CuAl_2(s) + 6H_2O(l) + 2OH^-(aq) = Cu(s) + 2Al(OH)_4^-(aq) + 3H_2(g) \quad (8)$$

and therefore

$$X_{Al} = \frac{V_{H_2(t)}}{V_{H_2(\text{complete extraction})}} \quad (9)$$

where V_{H_2} is volume of hydrogen evolved at experimental conditions. Thus X_{Al} can readily be obtained with a high degree of accuracy either by chemical analysis of the alloy and catalysts (Eq. (6)) or by monitoring hydrogen evolution for partially and fully leached alloy samples (Eq. (9)). Furthermore, since the index X_{Al} is only dependent on the extent to which leaching has progressed in the alloy, it can be applied to any particle geometry.

Additional experiments were carried out on alloy particles of different sizes. The same temperature and caustic addition techniques were employed, but the alloy particles were leached to completion, i.e., $X_{Al} = 1$. A separate alloy melt was made for these experiments. Its composition was Cu–48 wt% Al and the particle size ranges employed are given in Table 3.

RESULTS AND DISCUSSION

Leaching Kinetics

The volumes of hydrogen evolved during the preparation of the various catalysts are plotted as a function of time in Fig. 2. A comparison of the measured evolution of hydrogen with that attributed to lost aluminium (Table 1) shows that hydrogen evo-

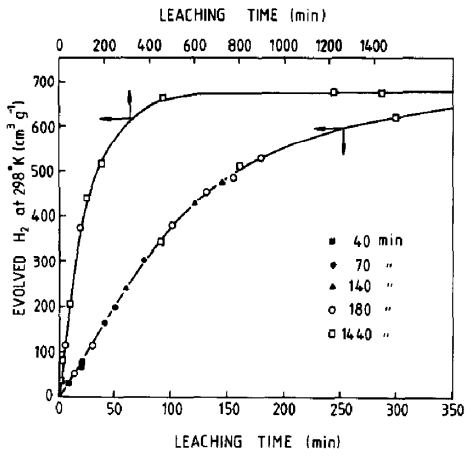

FIG. 2. Hydrogen evolution during caustic leaching of $CuAl_2$ alloy. Symbols represent experimental hydrogen evolutions during extractions conducted over different total times.

lution is a direct measure of the removal of aluminium from the alloy. The plot of hydrogen evolution against leaching time shown in Fig. 2 is essentially linear over the first 60 min of leaching (X_{Al} = 0.36) after which the rate progressively decreases. As a result of the method of alkali additions, caustic concentration is usually much higher during the later part of the extraction than at the beginning. The decrease in leaching rate cannot therefore be attributed to a decrease in caustic concentration.

From Fig. 2 it is apparent that reaction is complete after 500 min at which time 670 cm^3 of hydrogen has been evolved, this being equivalent to the removal of all leachable aluminium from the alloy. Levenspiel (*18*) has considered the case of spherical particles of unchanging size reacting in a fluid. There are 3 particular cases of the unreacted core model to consider and these are:

1. Diffusion through the liquid film controls the rate.
2. Diffusion through the reacted rim (shell) controls the rate.
3. Chemical reaction at the core/shell interface controls the rate.

For spherical particles when the time for complete reaction is given by τ, we can write the relationship between dimensionless time t/τ and the conversion of the aluminium X_{Al} for the three cases as

$$\frac{t}{\tau} = X_{Al} \qquad \text{for liquid film diffusion control}$$

$$\frac{t}{\tau} = 1 - 3(1 - X_{Al})^{2/3} + 2(1 - X_{Al}) \qquad \text{for diffusion through the shell control}$$

$$\frac{t}{\tau} = 1 - (1 - X_{Al})^{1/3} \qquad \text{for chemical reaction control.}$$

These generalized equations are plotted in Fig. 3. Also plotted in Fig. 3 are the experimental values of $1 - X_{Al}$ and t/τ calculated from the hydrogen evolution curves in Fig. 2. The results in Fig. 3 show that the leaching of the alloy is chemical reaction controlled for the first 25 min corresponding to X_{Al} = 0.13; between 25 and 200 min (corresponding to X_{Al} in the region of 0.13 to 0.44) the reaction is limited by diffusion through the reaction rim. After that time the reaction is completely diffusion controlled.

Surface Area and Pore Development

Experimental results on the surface areas and pore structure of the catalysts were ob-

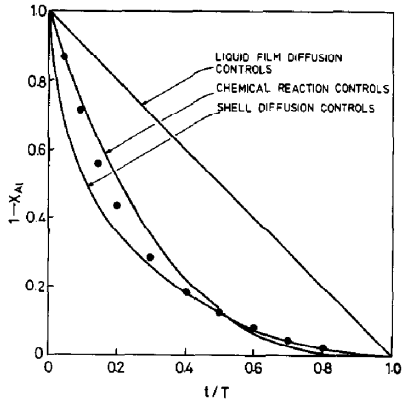

FIG. 3. Plots of generalized shell model equations for chemical reaction and diffusion controlled reaction of a spherical particle with unchanging size and shrinking core (*18*). Lines represent generalized model curves. ●, Experimental points.

TABLE 2

Surface Area and Pore Structure Data for Varying Times of Extraction

Extraction			Surface areas[a] ($m^2\ g^{-1}$)			Pore volumes[a] ($cm^3\ g^{-1}$)			Pore radii (Å)[b]		Interpore distance (Å)
Time (min)	Extent X_{Al}	Depth (mm)	S_c	S_s	S_m	ν_c	ν_s	ν_m	r_p	r_a	
40	0.22	0.085	4.54	37.6	4.1	0.029	0.24	0.026	128	128	132
70	0.42	0.20	9.6	36.6	7.6	0.060	0.25	0.048	137	125	139
140	0.64	0.33	12.6	26.1	8.3	0.12	0.24	0.077	214	190	221
180	0.75	0.40	13.9	23.5	8.7	0.16	0.27	0.10	240	230	235
1440	1.0	1.09	15.3	15.5	7.7	0.24	0.24	0.12	321	314	331

[a] Subscripts: c, per unit mass of composite particle; s, per unit mass of shell; m, per unit mass of initial alloy particle.

[b] r_p values correspond to the maxima in the plot of $\Delta\nu_c/\Delta r_p$ in Fig. 4. r_a is the "average" pore radius, which is given by $2\nu_c/S_c$.

tained on the basis of unit mass of the composite material. These are presented in Table 2. Also presented are properties based on a unit mass of shell as calculated from Eq. (3), and unit mass of starting alloy particle.

The pore size distributions of particles extracted for different periods of time are plotted in Fig. 4. The volumes of pores in the catalysts were evaluated from the isotherms and are expressed per unit mass of composite material. From Fig. 5 it can be seen that for a given mass (and hence volume) of alloy the volume created in the pores is directly proportional to the amount of aluminium removed. The value of the pore radius, r_p, at which a maximum in the differential pore volume is encountered is clearly defined in Fig. 4. This value becomes progressively larger with X_{Al} as shown in Fig. 6. An average pore radius, $r_a = 2V_{0.95}/S_{BET}$, is calculated in Table 2 where it also is seen to increase with X_{Al}.

These results, taken alone, are susceptible of two interpretations. They could indi-

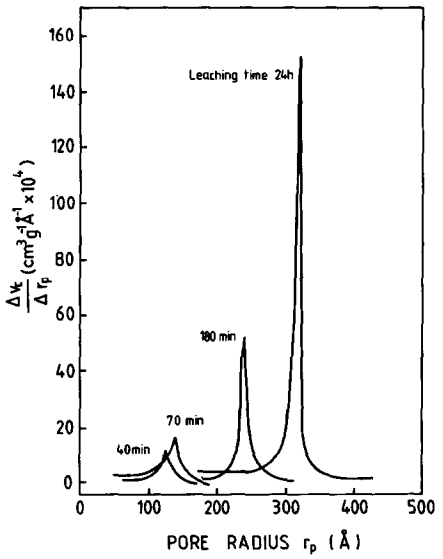

FIG. 4. Variation in pore size distribution during caustic leaching of the alloy.

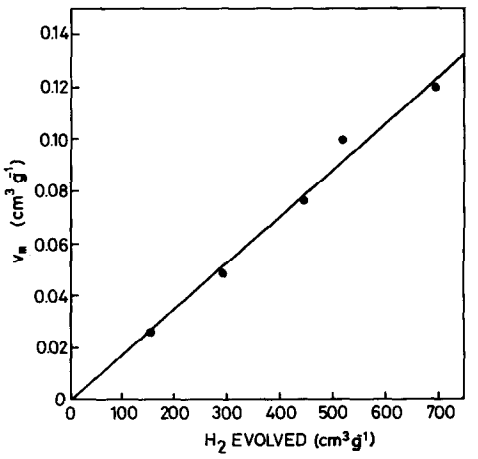

FIG. 5. Development of internal (pore) volume in Raney copper during caustic extraction of the alloy.

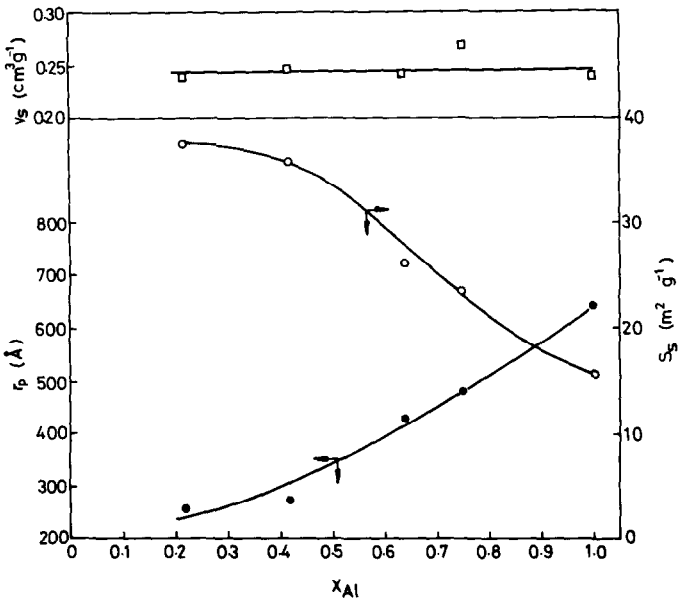

FIG. 6. Variation of pore volume, pore diameter and surface area in the active shell of the Raney foraminate catalyst.

cate that pores in the reacted rim continue to enlarge as reaction proceeds. An alternative interpretation is that pores, once formed, are stable in dimension but that new pores formed at an advanced stage of reaction are larger than those formed earlier, thus weighting the measured average toward progressively higher values. An enlargement of already existing pores would require either further leaching of aluminium from the surrounding copper, or a sintering process. Further leaching is insignificant because only very low concentrations of aluminium are ever found in the copper residue. Sintering of the copper seems highly unlikely given the low temperature and the fact that the space between the copper particles is occupied by a liquid in which copper is essentially insoluble. The pore enlargement hypothesis is therefore rejected. The remaining possibility of a progressive change with time in reaction morphology at the leach reaction front receives support from a consideration of diffusion mechanisms, as discussed below.

Figure 6 shows that the catalyst surface area per unit mass of the skeletal shell decreases progressively with the extent of leaching. Figure 6 also shows that the pore volume per unit mass of the shell remains essentially constant at a value of 0.25 cm^3 g^{-1} over the entire extraction. These observations are consistent with the formation at the early stage of extraction of a large number of small pores, and an enlargement of average pore size as extraction progresses due to the formation of additional large pores.

The values of the BET surface area per unit mass of starting alloy are presented for various times of extraction in Table 2. These results show that the internal surface area produced per unit mass of alloy increases with increased extent of leaching to attain a maximum value after about 180 min of leaching with a slight reduction in area at greater extents of extraction. This maximum results from the fact that both pore volume and pore radius increase monotonically with X_{Al}.

Comparison with Completely Extracted Particles

Data obtained for leached foraminate shells of various thicknesses may be compared to that for fully leached particles of various sizes. Referring to Table 3, it is seen that the BET surface area per unit mass decreases with increasing particle size. The BET surface area per unit mass of shell (Table 2) also decreases as the shell thickness increases. Similarly, average pore diameters increase both with the size of fully leached particles and with the shell thickness of foraminates. In all cases the pore volume of the leached material is approximately constant since the dissolution of aluminium is close to quantitative. The changes in surface area and pore diameter are therefore manifestations of the same effect: pores become larger and more widely spaced as the depth of leaching increases. This behavior may be understood in terms of the mechanism of copper–aluminium segregation within the alloy at the leach reaction front.

Diffusion Model for Pore Development

The variation in the leaching time in the formation of the foraminate catalysts affects the pore structure of the catalyst rim. As the pore size and interpore distance are determined by diffusion of the alloy constituents it is important to determine how rearrangement occurs within the solid to accommodate the loss of two-thirds of its constituent atoms in reaction (*8*). The process is presented schematically in Fig. 7. Segregation of the constituent elements of the alloy toward the advancing reaction front can occur by diffusion within the parent phase or by diffusion along the interface between the parent and product phases.

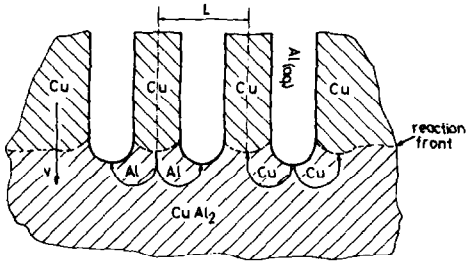

FIG. 7. Schematic representation of a $CuAl_2$–Cu grain and the alloy–reaction product interface (*12*).

Because the reaction kinetics are diffusion controlled and therefore parabolic, leaching the alloy particles for increasing periods of time corresponds to a decrease in the average reaction rate for the formation of the catalyst rim. The decrease in the average reaction rate results in an increase in the average diffusion distance of the alloy constituents, $\bar{L}$, where L is the sum of pore width, L^P and remnant copper trunk width, L^{Cu}.

Expressions relating the diffusion distance to the velocity, v, at which the reaction front advances into the parent phase have been developed (*12*). For volume diffusion the result is

$$v = \frac{2D}{af^{Cu}f^{P}RT} \cdot \frac{\sigma^{CuP}}{C^{Cu}} \cdot \frac{1}{\bar{L}^2} \qquad (10)$$

where D is the solid-state chemical diffusion coefficient in $CuAl_2$, a is a geometric constant of order unity, f^{Cu} and f^P are the ratios L^{Cu}/L and L^P/L and are determined by the parent phase composition, σ^{CuP} is the surface energy of the Cu-pore phase boundary, C^{Cu} is the concentration of the copper, R is the gas constant, and T is temperature.

The relationship for boundary diffusion is

TABLE 3

Surface and Pore Structure Data for Particles of Cu–48 wt% Al Alloy Fully Leached at 313 K

Particle size (mm)	S_c ($m^2\ g^{-1}$)	v_c ($cm^3\ g^{-1}$)	Pore radii (Å)		Interpore distance (Å)
			r_p	r_a	
0.35–0.42	27.0	0.25	159	185	161
0.71–0.85	21.3	0.25	171	235	176
1.00–1.18	20.2	0.23	179	228	189
1.40–1.68	20.3	0.19	213	246	247
2.00–2.36	18.6	0.17	201	269	247

$$v = \frac{24 D_B \delta K f^{Cu} f^P \sigma^{CuP}}{aRTC^{Cu}} \cdot \frac{1}{L^3} \qquad (11)$$

where D_B is the boundary diffusion coefficient, δ is the boundary width, and K is the coefficient representing partition of solute between bulk $CuAl_2$ and boundary. Since the measurements of pore diameter were obtained from the entire sample they represent volume averages. It is necessary to relate these averages to the instantaneous quantities. By definition

$$\overline{L^2} = \frac{\int L^2 dV}{\int dv}$$

where V represents volume. For spherical particles of radius R_P with an unreacted alloy core of radius R_C

$$\overline{L^2} = 3 \int_{R_C}^{R_P} L^2 r^2 dr / (R_P^3 - R_C^3) \qquad (12)$$

where r is the radial coordinate within the sphere.

From Eq. (10) the diffusion distance is related to the volume diffusion coefficient and the velocity of the reaction front by

$$L^2 = \frac{\kappa D}{v} \qquad (13)$$

where $\kappa = 2\sigma^{CuP}/f^{Cu} f^P aRTC^{Cu}$. As the reaction was found to have parabolic leaching kinetics (*12*) it follows that

$$v = \frac{dX}{dt} = \frac{k_p}{2X} \qquad (14)$$

where k_p is the parabolic rate constant and X is the thickness of reaction product rim. Combining these two equations yields

$$L^2 = \frac{2\kappa D X}{k_p}$$

which for a spherical particle becomes

$$L^2 = \frac{2\kappa D (R_p - r)}{k_p}. \qquad (15)$$

Using X_{Al} as a measure of leaching, V_p = volume of original (spherical) particle, and V_c = volume of unleached core after given time of leaching then

$$\frac{V_c}{V_p} = 1 - X_{Al} \qquad r = R_p(1 - X_{Al})^{1/3}. \qquad (16)$$

Combination of Eqs. (12), (15), and (16) followed by integration yields

$$\overline{L^2} = \frac{\kappa D}{2k_p} \frac{R_p}{X_{Al}} [4X_{Al} - 3 + 3(1 - X_{Al})^{4/3}]. \qquad (17)$$

The corresponding expression for boundary diffusion is

$$\overline{L^3} = \frac{\kappa^1 D_B \delta K R_p}{2k_p X_{Al}} [4X_{Al} - 3 + 3(1 - X_{Al})^{4/3}] \qquad (18)$$

where $\kappa^1 = 24 f^{Cu} f^P \sigma^{CuP}/aRTC^{Cu}$. Equations (17) and (18) predict a simple dependency of $\overline{L}$ on R which has been verified (*12*) for the case $X_{Al} = 1$.

The pore diameter, $\overline{L^P}$, and the copper width, $\overline{L^{Cu}}$, are required to calculate $\overline{L}$. The quantity $\overline{L^{Cu}}$ is calculated from the pore volume and $\overline{L^P}$, on the presumption that the pores are uniform, cylindrical, and parallel. Assuming that the pore axes are arrayed on a square grid and that the intervening regions of solid are composed of pure copper,

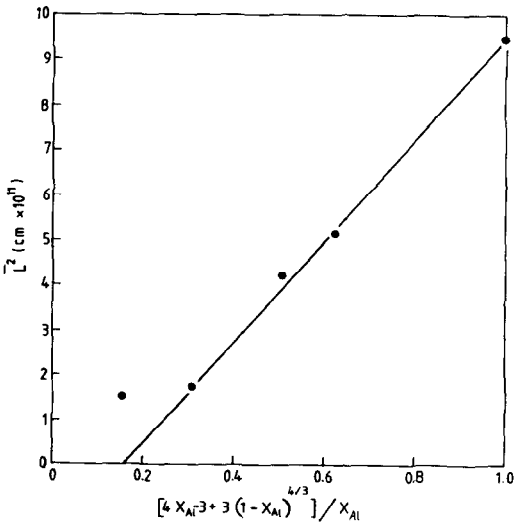

FIG. 8. Plot of Eq. (17).

the average interpore distances shown in Table 3 are calculated.

The data are plotted according to Eq. (17) in Fig. 8. A value for D is calculated from the slope using the values $a = 1, f^{Cu} = 0.36$, $f^{P} = 0.64$, $\sigma^{CuP} = 300$ erg cm^{-2}, $C^{Cu} = 0.13$ mol cm^{-3}, and $k_p = 7.25 \times 10^{-8}$ cm^2 s^{-1}. The value obtained is $D = 1 \times 10^{-10}$ cm^2 s^{-1}. This is in reasonable agreement with the value of 2×10^{-11} cm^2 s^{-1} calculated from the value obtained at 293 K for fully leached particles (*12*) using the measured activation energy.

If alloy segregation occurs via boundary diffusion, then Eq. (18) applies. In this case the slope of the plot shown in Fig. 9 leads to the estimate

$$D_B \delta K = 4 \times 10^{-15} \text{ cm}^3 \text{ s}^{-1}.$$

Using the estimates $\delta = 10$ Å and $K = 2$, it is found that $D_B = 2 \times 10^{-8}$ cm^2 s^{-1} which also agrees reasonably well with the value of 4×10^{-9} cm^2 s^{-1} calculated from data obtained from fully leached particles (*12*).

The value for D obtained from the volume diffusion mechanism is enormously higher than the value calculated by extrapolation of high temperature data (*19*) but is in agreement with a value of 1×10^{-12} cm^2 s^{-1} deduced by Pickering and Wagner (*20*) for diffusion of copper in a copper–gold alloy at 25°C and attributed to a divacancy mechanism. Such a mechanism might be operative in the present case but no independent evidence for it exists.

It is difficult to comment on the value of boundary diffusion coefficient in the absence of information on the $CuAl_2$/Cu boundary diffusion properties. However activation energies calculated from data on fully leached particles show clearly that volume diffusion cannot be operative, and that alloy segregation occurs by a mechanism of boundary diffusion (*12*).

It has been demonstrated that a decrease in leach reaction rate leads to an increase in pore spacing. One method of controlling the average leaching rate is through control of the degree of extraction for alloy particles of a given size. Catalysts having a variety of pore structures can be produced in this way. Control of pore structure is important in the Raney copper catalyzed hydrolysis of acrylonitrile (*13*) and can be achieved by varying the leaching temperature, concentration and through the use of chemical additives to the leach liquor (*21*).

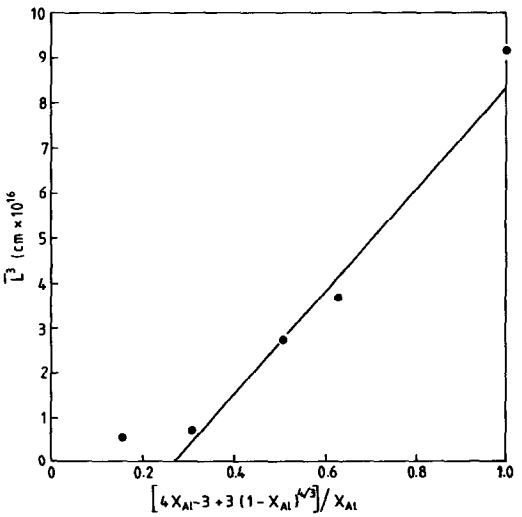

FIG. 9. Plot of Eq. (18).

ACKNOWLEDGMENT

The authors gratefully acknowledge financial support of the Australian Research Grants Scheme.

REFERENCES

1. Matsuda, F., *Chemtech.* **7,** 306 (1977).
2. Mitsui Toatsu, Japan Appl. 71/62, 558 (19 July 1971).
3. Mitsui Toatsu, Ger. Off. 2,240,783 (22 Feb. 1973).
4. Werges, D. L., Belg. Patent 817,648 (1975).
5. Svarz, J. J., Goretta, L. A., and Searle, V. L., U.S. Patent 4,914,820 (1971).
6. Elsemongy, M. M., and Onsager, O. T., *Acta. Chem. Scand. B* **32,** 167 (1978).
7. Wainwright, M. S., Onuoha, N. I., and Chaplin, R. P., Proc. 7th Aust. Conf. Chem. Eng. 109 (Aug. 1979).
8. Onuoha, N. I., and Wainwright, M. S., *Chem. Eng. Commun.* **29,** 1 (1984).
9. Onuoha, N. I., and Wainwright, M. S., *Chem. Eng. Commun.* **29,** 13 (1984).
10. Reynolds, P. W., *J. Chem. Soc.* 265 (1950).
11. Friedrich, J. B., Young, D. J., and Wainwright, M. S., *J. Catal.* **80,** 14 (1983).

12. Tomsett, A. D., Young, D. J., and Wainwright, M. S., *J. Electrochem. Soc.* **131,** 2476 (1984).
13. Onuoha, N. I., Ph.D. Thesis, University of New South Wales (1983).
14. Pierce, C., *J. Phys. Chem.* **57,** 149 (1953).
15. Orr, C., and Dalla Valle, J. M., "Fine Particle Measurement," p. 271. Macmillan and Co., London, 1959.
16. Wainwright, M. S., and Anderson, R. B., *J. Catal.* **64,** 124 (1980).
17. Friedrich, J. B., Wainwright, M. S., and Young, D. J., *J. Catal.* **80,** 1 (1983).
18. Levenspiel, O., "Chemical Reaction Engineering," 2nd Ed., John Wiley, New York, 1975.
19. Smithells, C. J., "Metals Reference Book," Vol. II. Butterworths, London, 1955.
20. Pickering, H. W., and Wagner, C., *J. Electrochem. Soc.* **114,** 698 (1967).
21. Tomsett, A. D., Wainwright, M. S., and Young, D. J. (unpublished data).